Journal of Solid State Chemistry **145,** 564–572 (1999)
Article ID jssc.1999.8222, available online at http://www.idealibrary.com on IDEAL®

Stable Two-Dimensional Metallic State with Stacking Motif of "Spanning Overlap" in γ-$[(CH_3)_2(C_2H_5)_2N][Ni(dmit)_2]_2$

Akiko Kobayashi,* Akane Sato,† and Hayao Kobayashi†

*The University of Tokyo, Hongo, Bunkyo-ku, Tokyo 113-0033, Japan; and †Institute for Molecular Science, Okazaki 444-8585, Japan

Received October 9, 1998; in revised form February 10, 1999; accepted February 11, 1999

THE AUTHORS DEDICATE THIS ARTICLE TO PROFESSOR PETER DAY, HONOURING HIS WORK IN THE AREAS OF SOLID STATE AND MATERIALS CHEMISTRY ON THE OCCASION OF HIS 60TH BIRTHDAY

The crystal structure of γ-$[(CH_3)_2(C_2H_5)_2N][Ni(dmit)_2]_2$, $Ni_2S_{20}C_{18}NH_{16}$ was determined by use of a four-circle diffractometer (at 294 K) and imaging plate (IP) system equipped with a He refrigerator (7 K). Crystal data: at 294 K, orthorhombic *Pnma*, $a = 14.014(4)$ Å, $b = 37.072(13)$ Å, $c = 6.519(2)$ Å, $V = 3386.8(1.8)$ Å^3, $Z = 4$, $R(Rw) = 0.066(0.051)$ for 1284 reflections; at 7 K, orthorhombic $P2_12_12_1$, $a = 13.760(45)$ Å, $b = 36.622(77)$ Å, $c = 6.500(2)$ Å, $V = 3275.5(1.4)$ Å^3, $Z = 4$, $R(Rw) = 0.062(0.077)$ for 3064 reflections. The magnetic susceptibility measurement of γ-$[(CH_3)_2(C_2H_5)_2N][Ni(dmit)_2]_2$ showed that it was metallic down to 2 K with the Pauli-like magnetic susceptibility. This susceptibility behavior is quite different from that of the isomorphous α-$[(CH_3)_2(C_2H_5)_2N][Ni(dmit)_2]_2$. The tight-binding band structure calculation by extended Hückel methods indicated that γ-$[(CH_3)_2(C_2H_5)_2N][Ni(dmit)_2]_2$ has the round two-dimensional Fermi surfaces at 7 K. The conductivity measurements showed no sign of the superconducting transition down to 0.1 K.

***Key Words*: molecular superconductor; molecular metal; dmit compounds; spanning overlap; crystal structure; low-temperature crystal structure; two-dimensional metal.**

INTRODUCTION

From the viewpoint of molecular design, there are some important future targets of the chemistry of molecular conductors; for example, an ambient-pressure π-acceptor superconductor with closed-shell cations is one of them. Among molecular metals based on π-acceptor molecules, $M(dmit)_2$ has played an important role in the development of new molecular conducting systems. Eight molecular superconductors have been discovered in $M(dmit)_2$ salts (1–8). However, until 1993, all the known ambient-pressure superconductors were based on TTF-like planar π donors (7). A simple approach to an ambient-pressure "pure π-acceptor superconductor" without π-donor molecules might be to design π-acceptor conductors with stable metallic states down to low temperature. From this viewpoint, two candidates were considered around the beginning of the 1990s. One was α-(EDT-TTF)$[Ni(dmit)_2]$, because of the observation of a decreasing electrical resistivity down to 1.5 K, after taking a maximum around 14 K (7). Meanwhile, in 1993, the superconducting transition was in fact found at 1.3 K at ambient pressure. The resistivity anomaly around 14 K was assigned to the CDW or SDW formation within the EDT-TTF chain by the reflection spectra, weak-field magnetoresistance, and electrical resistivity measurements. As mentioned before, this was the first ambient-pressure superconductor in a series of $M(dmit)_2$ salts [M = Ni, Pd, Pt, Au, ….].

The other group of candidates of an ambient pressure superconductor is $[(CH_3)_2(C_2H_5)_2N][Ni(dmit)_2]_2$ (9), which has polymorphs α, β, and γ. α-$[(CH_3)_2(C_2H_5)_2N][Ni(dmit)_2]_2$ (10) and γ-$[(CH_3)_2(C_2H_5)_2N][Ni(dmit)_2]_2$ (11) are novel transition metal compounds which retain metallic conductivity down to low temperature. We expected these compounds to be candidates of the first ambient-pressure pure π-acceptor superconductors based on $Ni(dmit)_2$ and closed-shell cations. The reason is the large two-dimensional Fermi surface obtained from the electronic band structure calculation, based on the room temperature structure. However, in the case of α-salt, the tight-binding band calculation basesd on the low-temperature structure showed that many pieces of complicated small Fermi surfaces appeared at low temperature owing to the structural phase transitions. And no sign of the superconducting transition was obtained down to 0.1 K.

In this paper the low-temperature crystal structure, electrical resistivity, magnetic susceptibility, and the tight-binding band structure of γ-$[(CH_3)_2(C_2H_5)_2N][Ni(dmit)_2]_2$ are described.

0022-4596/99 $30.00

EXPERIMENTAL

Synthesis

Black plate crystals of $[(CH_3)_2(C_2H_5)_2N][Ni(dmit)_2]_2$ were prepared electrochemically. X-ray examination showed the existence of three modifications (α, β, γ). The solvents were reagent grade and freshly distilled. $[(CH_3)_2(C_2H_5)_2N]_2[Ni(dmit)_2]$ was prepared according to the literature methods. α-Type crystals were grown as plate crystals by electrochemical oxidation from the mixed solvent of 50% acetone and 50% acetonitrile (15 ml) containing $[(CH_3)_2(C_2H_5)_2N]_2[Ni(dmit)_2]$ (12.7 mg) and $[(CH_3)_2(C_2H_5)_2N]ClO_4$ (60 mg). γ-Type crystals were grown as plate crystals by electrochemical oxidation from acetonitrile (15 ml) containing $[(CH_3)_2(C_2H_5)_2N]_2[Ni(dmit)_2]$ (11.0 mg) and $[(CH_3)_2(C_2H_5)_2N]ClO_4$(53.2 mg). The constant current of 1–2 μA was applied for 7–14 days. The H-shape glass cells were used. β-Type crystals were grown as black elongated plates, which belong to the monoclinic system with the space group of $P2_1/c$ and the lattice constants of $a = 27.685$ Å, $b = 7.845$, $c = 11.508$, and $\beta = 101.33°$. However, further investigation is not made because it is a semiconductor.

Crystal Structure Determination

The X-ray data at 294 K were obtained by a four-circle diffractometer equipped with a rotating anode (Rigaku AFC-5R). Crystal data and experimental details are listed in Table 1. The atomic parameters are listed in Table 2. The empirical absorption corrections were made. All the calculations were performed using the teXsan crystallographic software package (12). The crystal structure determination at 7 K was performed by a Weissenberg-type imaging plate system (Mac Science DIP-320) with a helium refrigerator (13). Crystal data and experimental details at 7 K are listed in Table 3. Monochromated Mo$K\alpha$ radiation ($\lambda =$ 0.7107 Å) was used in all the X-ray experiments. The structure was solved by direct methods. All the nonhydrogen atoms were refined anisotropically using the program ANYBLK (14). The atomic parameters at 7 K are listed in Table 4.

Electronic Band Structure Calculation

The electronic band structures were calculated by using an extended Hückel tight-binding approximation on the basis of the lowest unoccupied molecular orbitals (LUMO) and the highest occupied molecular orbitals (HOMO) of $Ni(dmit)_2$ (15). The exponents ζ and ionization potentials (eV) for atomic orbitals are listed in Table 5.

TABLE 1
Crystal Data and Experimental Details for γ-$[(CH_3)_2(C_2H_5)_2N][Ni(dmit)_2]_2$ at 294 K

Chemical formula	$Ni_2S_{20}C_{18}NH_{16}$
Temperature	294 K
Formula weight	1005.04
a (Å)	14.014(4)
b (Å)	37.072(13)
c (Å)	6.519(2)
V (Å^3)	3386.8(1.8)
Space group	*Pnma*
Z	4
F (000)	2028.00
d_{calc} (g cm^{-3})	1.972
Dimensions (mm)	$0.18 \times 0.100 \times 0.03$
Radiation	Mo($K\alpha$) (0.71069 Å)
Data collection	AFC5R diffractometer
Scan type	ω
Scan width	$(0.756 + 0.300\tan\theta)°$
μ cm^{-1}	23.03
Corrections	Lorentz polarization, absorption (0.855–1.000)
$2\theta_{max}$ (°)	55.0
Reflection	total, 4599; unique, 4503
Reflection used ($I > 3.0\sigma$)	1284
R, R_w	0.066, 0.051
g.o.f.	1.99
Refinement	full-matrix least-squares
Weighting scheme	$4F^2/\sigma^2$
Max. shift/error in Final cycle	0.02
Max. peak in final Diff. map	0.85 e/Å^3
Min. peak in final	-0.83 e/Å^3

Physical Properties

The electrical resistivities were measured along the direction parallel to (010) by the conventional four-probe method from room temperature to 0.5 K. The resistivities were also examined down to 0.1 K to examine the possibility of the superconducting transition. Gold wires (0.015 (or 0.01) mmϕ) were bonded to the crystals with conducting gold paint.

The measurements of magnetic susceptibilities were performed on a SQUID (Quantum design MPMS-5 and MPMS-2) from 300 to 2 K by using polycrystalline samples.

RESULTS AND DISCUSSIONS

Resistivities of γ-$[(CH_3)_2(C_2H_5)_2N][Ni(dmit)_2]_2$

As mentioned before, the resistivity measurements showed that the γ-type crystals are metallic down to low temperature. When we found the metallic crystals of $[(CH_3)_2(C_2H_5)_2N][Ni(dmit)_2]_2$, we did not note the existence of polymorphic forms (9) and erroneously reported the

TABLE 2
Atomic Coordinates and B_{iso} of γ-$[(CH_3)_2(C_2H_5)_2N][Ni(dmit)_2]_2$ at 294 K

	x	y	z	B_{iso}	Occ.
Ni1	0.1113(1)	0.02041(5)	0.1281(3)	2.37(4)	1.0
S1	0.1018(3)	0.04843(10)	− 0.1601(6)	2.66(9)	1.0
S2	0.0711(3)	0.0673(1)	0.3025(6)	3.20(10)	1.0
S3	0.1570(3)	− 0.0269(1)	− 0.0403(6)	2.93(9)	1.0
S4	0.1179(3)	− 0.00754(10)	0.4170(5)	2.91(9)	1.0
S5	0.0474(3)	0.1259(1)	− 0.2594(6)	2.92(9)	1.0
S6	0.0167(3)	0.1428(1)	0.1681(6)	3.6(1)	1.0
S7	0.2044(3)	− 0.1023(1)	0.1026(7)	3.05(10)	1.0
S8	0.1668(3)	− 0.0839(1)	0.5254(6)	3.15(10)	1.0
S9	− 0.0048(4)	0.2006(1)	− 0.1398(8)	4.7(1)	1.0
S10	0.2199(4)	− 0.1586(1)	0.4265(8)	4.9(1)	1.0
N1	0.210(2)	0.2500	0.405(4)	9.3(8)	0.5
C1	0.067(1)	0.0908(4)	− 0.086(2)	2.6(3)	1.0
C2	0.055(1)	0.0988(4)	0.113(2)	2.7(3)	1.0
C3	0.1711(9)	− 0.0582(3)	0.150(2)	2.1(3)	1.0
C4	0.154(1)	− 0.0500(4)	0.354(2)	2.9(3)	1.0
C5	0.017(1)	0.1588(4)	− 0.080(2)	3.1(3)	1.0
C6	0.197(1)	− 0.1173(4)	0.354(2)	2.8(3)	1.0
C7	0.233(2)	0.2500	0.158(5)	8.2(9)	0.5
C8	0.338(2)	0.2500	0.137(5)	8.5(9)	0.5
C9	0.089(2)	0.2500	0.341(5)	9.4(10)	0.5
C10	0.214(2)	0.2018(6)	0.437(3)	8.5(7)	1.0

temperature dependence of the resistivity of the γ-crystal to be that of the α-crystal. It was reported that the resistivity of α-$[(CH_3)_2(C_2H_5)_2N][Ni(dmit)_2]_2$ shows a discontinuous drop (or jump) around 240 K, where the unit cell volume discontinuously decreases by about 40 Å^3 (10). The room temperature conductivity of γ-$[(CH_3)_2(C_2H_5)_2N][Ni(dmit)_2]_2$ is 10–100 S cm^{-1}. As seen from Fig. 1, the resistivity of γ-$[(CH_3)_2(C_2H_5)_2N][Ni(dmit)_2]_2$ exhibited a smooth decrease around 240 K. However, the resistivity frequently showed a small anomaly around 100 K, which will be related to the structural transformation around this temperature region as mentioned later. The resistivity was measured on two samples down to 0.1 K to examine the possibility of the superconductivity. However, as in the case of α-type crystals, no sign of superconductivity was obtained.

Crystal Structure

The crystal structure of γ-$[(CH_3)_2(C_2H_5)_2N][Ni(dmit)_2]_2$ at room temperature is shown in Fig. 2. The crystal does not take a simple one-dimensional column structure. Along the c-axis, $Ni(dmit)_2$ molecules are arranged in a side-by-side fashion with short S–S distances. Along the a direction. $Ni(dmit)_2$ molecules form a dimer and one of the dimer molecules overlaps with the upper two molecules. That is, the crystal has a "spanning overlap molecular arrangement," which was first found in α-$[(CH_3)_2(C_2H_5)_2N][Ni(dmit)_2]_2$. The spanning overlap molecular arrangement is shown in Fig. 3. The $(CH_3)_2(C_2H_5)_2N$ cations are on the mirror plane and are heavily disordered. The C and N atoms could not be located in the structure analysis. The crystal structure at 7 K is shown in Fig. 4. The space group of *Pnma* of the high-temperature phase is changed to $P2_12_12_1$ at low temperature. Considering the disordered conformation of $(CH_3)_2(C_2H_5)_2N$ located on the mirror plane at room temperature, the change of the lattice symmetry will be related to the order-disorder transition of the $(CH_3)_2(C_2H_5)_2N$ group. In contrast to the case of α-$[(CH_3)_2(C_2H_5)_2N][Ni(dmit)_2]_2$, the cell parameters at 294 and 7 K listed in Tables 1 and 3 indicated that the structural change is not so large. The lattice contractions were almost the same along the a, b, and c directions ($\Delta a/a$, $\Delta b/b$, and $\Delta c/c$ 0.3 ~ 1.8%) (see also Fig. 5). At 7 K, the $(CH_3)_2(C_2H_5)_2N$ cations are on the general positions and all the C and N atoms of the cations are ordered. At the same time, two $Ni(dmit)_2$ molecules became crystallographically independent.

The bond lengths and angles at 294 and 7 K are listed in Tables 6 and 7. The $Ni(dmit)_2$ molecules are almost planar. The average bond lengths (r) and bond angles (θ) of the $Ni(dmit)_2$ molecules at 294 and at 7 K are as follows: at

TABLE 3
Crystal Data and Experimental Details for γ-$[(CH_3)_2(C_2H_5)_2N][Ni(dmit)_2]_2$ at 7 K

Chemical formula	$Ni_2S_{20}C_{18}NH_{16}$
Temperature	7 K
Formula weight	1005.04
a (Å)	13.760(45)
b (Å)	36.622(77)
c (Å)	6.500(2)
V (Å^3)	3275.5(1.4)
Space group	$P2_12_12_1$
Z	4
F (000)	2028.00
d_{calc} (g cm^{-3})	2.038
Dimensions (mm)	$0.35 \times 0.25 \times 0.1$
Radiation	Mo($K\alpha$) (0.71069 Å)
Data collection	I P
μ cm^{-1}	23.78
$2\theta_{max}$ (°)	61.0
Reflection	total: 11798
Reflection used ($F > 4.0\sigma$)	3064
R, R_w	0.062, 0.077
g.o.f.	2.0
Refinement	full-matrix least-squares
Weighting scheme	$1/\sigma^2$
Max. shift/error in Final cycle	0.02
Max. peak in final Diff. map	1.24 e/Å^3
Min. peak in final	− 1.40 e/Å^3

TABLE 4
Atomic Coordinates and B_{iso} of γ-$[(CH_3)_2(C_2H_5)_2N][Ni(dimt)_2]$ at 7 K

	x	y	z	B_{iso}
Ni1	0.3876(8)	0.0183(1)	0.8489(9)	0.84(8)
Ni2	0.6095(4)	−0.0211(1)	0.5832(8)	0.83(8)
S1	0.3812(8)	−0.0102(2)	1.1384(16)	0.9(2)
S2	0.3402(8)	0.0293(2)	0.6787(17)	0.9(2)
S3	0.4313(8)	0.0652(2)	1.0272(17)	1.1(2)
S4	0.4006(7)	0.0471(2)	0.5581(16)	0.8(2)
S5	0.3273(8)	−0.0871(2)	1.2494(17)	1.0(2)
S6	0.2887(8)	−0.1056(2)	0.8225(17)	1.1(2)
S7	0.4953(8)	0.1406(2)	0.8958(17)	1.1(2)
S8	0.4610(8)	0.1253(2)	0.4643(17)	1.0(2)
S9	0.2707(8)	−0.1627(2)	1.1475(18)	1.1(2)
S10	0.5258(8)	0.1999(1)	0.5910(17)	1.0(2)
S11	0.5977(8)	−0.0489(2)	0.8740(17)	0.9(2)
S12	0.5663(8)	−0.0690(2)	0.4104(17)	1.0(2)
S13	0.6582(8)	0.0269(2)	0.7482(17)	1.0(2)
S14	0.6166(8)	0.0067(2)	0.2917(16)	1.0(2)
S15	0.5415(8)	−0.1273(2)	0.9774(17)	1.0(2)
S16	0.5090(8)	−0.1447(2)	0.5486(16)	1.0(2)
S17	0.7089(8)	0.1032(2)	0.5977(18)	1.0(2)
S18	0.6697(8)	0.0830(2)	0.1736(17)	1.0(2)
S19	0.4804(8)	−0.2028(2)	0.8628(17)	1.2(2)
S20	0.7242(8)	0.1592(2)	0.2638(18)	1.3(2)
C1	0.3434(33)	−0.0525(8)	1.0750(75)	1.3(4)
C2	0.3245(32)	−0.0609(7)	0.8686(71)	1.1(4)
C3	0.4545(31)	0.0967(7)	0.8362(71)	1.1(4)
C4	0.4370(31)	0.0896(7)	0.6391(74)	1.1(4)
C5	0.2941(30)	−0.1204(7)	1.0712(70)	1.2(4)
C6	0.4971(31)	0.1576(8)	0.6439(69)	1.2(4)
C7	0.5609(32)	−0.0924(8)	0.8073(73)	1.2(4)
C8	0.5474(28)	−0.1002(7)	0.6029(66)	0.6(4)
C9	0.6710(33)	0.0584(8)	0.5575(71)	1.3(4)
C10	0.6518(34)	0.0486(8)	0.3526(75)	1.5(4)
C11	0.5089(29)	−0.1605(7)	0.7972(64)	1.0(4)
C12	0.7016(31)	0.1178(8)	0.3351(73)	2.2(5)
N1	0.6712(27)	−0.2629(6)	0.3928(57)	1.6(3)
C13	0.5619(30)	−0.2604(8)	0.4111(67)	1.3(4)
C14	0.7013(30)	−0.3021(8)	0.3478(67)	1.4(4)
C15	0.7138(26)	−0.2515(8)	0.6078(61)	1.3(4)
C16	0.8222(29)	−0.2506(9)	0.6175(63)	1.7(5)
C17	0.7147(31)	−0.2397(7)	0.2229(69)	1.6(4)
C18	0.6946(30)	−0.1984(7)	0.2472(67)	1.4(4)

TABLE 5
The Exponents ζ and the Ionization Potentials (eV) for Atomic Orbitals

Orbital		ζ	E (eV)
S	3*s*	2.122	−20.0
	3*p*	1.825	−11.0
	3*d*	1.5	−5.44
Ni	4*s*	2.1	−7.34
	4*p*	2.1	−3.74
	4*d*	*	−10.6
C	2*s*	1.625	−21.4
	2*p*	1.625	−11.4

*Double ζ: 0.5681 $\chi_1(5.75)$ + 0.6294 $\chi_2(2.0)$.

294 K, r(Ni–S) = 2.155 Å, r(S–C) = 1.723 Å, r(C–C) = 1.36 Å, r(S–C(thione group)) = 1.625 Å, and θ(S–Ni–S) = 92.8°; at 7 K, r(Ni–S) = 2.161 Å, r(S–C) = 1.726 Å, r(C–C) = 1.375 Å, r(S–C (thione group)) = 1.638 Å and θ(S–Ni–S) = 92.78°. Tables 8 and 9 show the short intermolecular S ⋯ S contacts at 294 and 7 K. The shortest intermolecular S ⋯ S contact is 3.414 Å at 294 K and 3.48 Å at 7 K. The interplane distance within a dimer is 3.571 Å at 297 K and 3.478 Å at 7 K. The shortest intermolecular S ⋯ S short contact between terminal thioketone groups is 3.665 Å at 294 K and 3.576 Å at 7 K, which indicates that "three-dimensionality" is not strong in this system. The average C–C and C–N bond distances in the cation, which could not be determined at room temperature, are 1.52 and 1.533 Å, respectively, at 7 K. Besides the ordering of the cations, the low-temperature structure is essentially the same as the room-temperature structure.

In order to see the difference between the molecular overlaps of $Ni(dmit)_2$ in α-and γ-$[(CH_3)_2(C_2H_5)_2N][Ni(dmit)_2]_2$, the molecular overlaps of α- and γ-$[(CH_3)_2(C_2H_5)_2N][Ni(dmit)_2]$ are shown in Figs. 6a and 6b. The molecules within the dimer of γ-$[(CH_3)_2(C_2H_5)_2N][Ni(dmit)_2]_2$ are a little shifted with each other along the short axes of the molecules, while the molecular overlap in α-$[(CH_3)_2(C_2H_5)_2N][Ni(dmit)_2]_2$ at room temperature is a little different. The molecules are a little shifted along the long axes of the molecules. This slight difference produces

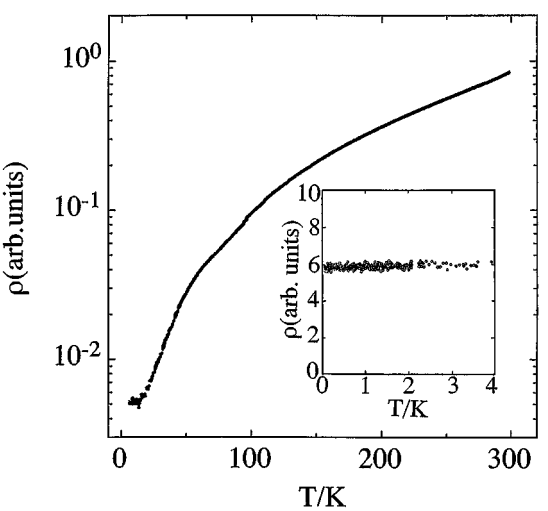

FIG. 1. Temperature dependence of the resistivity of γ-$[(CH_3)_2(C_2H_5)_2N][Ni(dmit)_2]_2$; details for the low temperature dependence are in the inset.

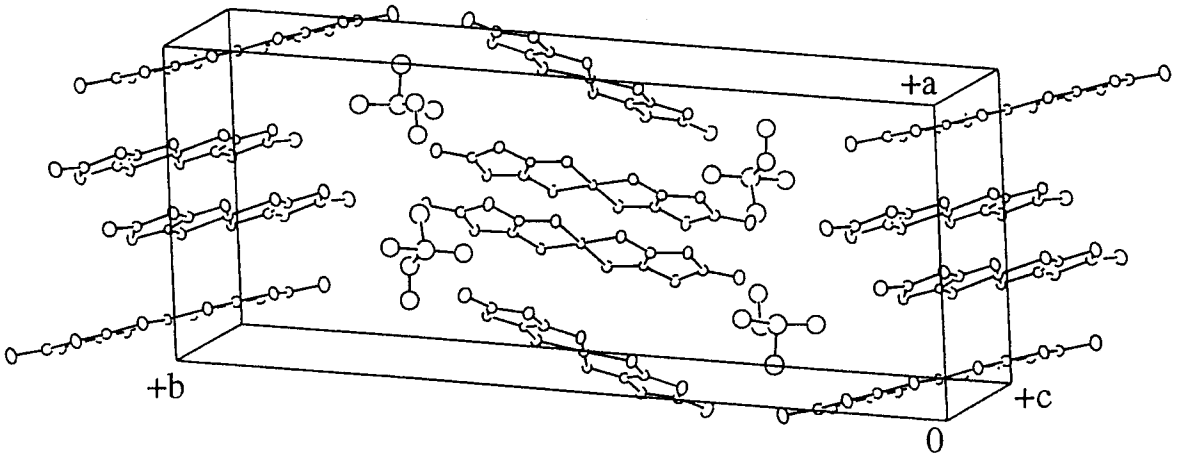

FIG. 2. The crystal structure of γ-$[(CH_3)_2(C_2H_5)_2N][Ni(dmit)_2]_2$ at 294 K. The thermal ellipsoids of ORTEP are drawn at the 30% probability level.

the fairly large differences in the two-dimensional Fermi surfaces of γ- and α-$[(CH_3)_2(C_2H_5)_2N][Ni(dmit)_2]_2$, which is mentioned later.

Magnetic Susceptibility

In the γ-salt, the Pauli-like almost temperature-independent magnetic susceptibility was observed above 120 K (Fig. 7). The diamagnetic contribution of $Ni(dmit)_2$ molecules were corrected using the diamagnetic susceptibilities of $[(CH_3)_4N]_2[Ni(dmit)_2$($\chi_{dia} = -2.7 \times 10^{-4}$ emu/mol), from which the diamagnetic susceptibility of $[(CH_3)_2(C_2H_5)_2N]$

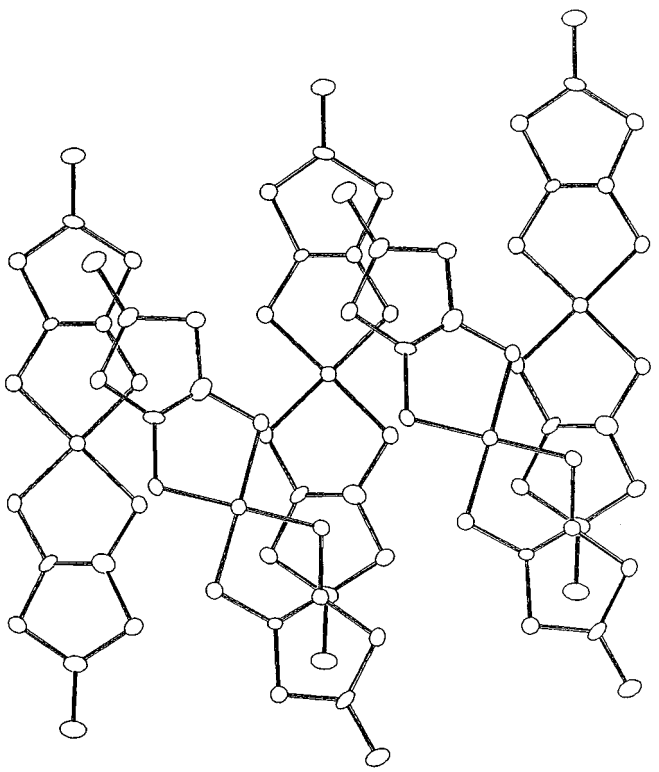

FIG. 3. The spanning overlap molecular arrangement, in γ-$[(CH_3)_2(C_2H_5)_2N][Ni(dmit)_2]_2$ at 294 K.

TABLE 6
Selected Bond Lengths (Å) and Angles (°) of γ-$[(CH_3)_2(C_2H_5)_2N][Ni(dmit)_2]_2$ at 294 K

Ni1–S1	2.151(4) Å	S5–C5	1.75(1) Å	N1–C7	1.64(4) Å
Ni1–S2	2.152(4)	S6–C2	1.75(1)	N1–C9	1.74(4)
Ni1–S3	2.64(4)	S6–C5	1.72(1)	N1–C10	1.80(2)
Ni1–S4	2.151(4)	S7–C3	1.73(1)	C1–C2	1.34(2)
S1–C1	1.71(1)	S7–C6	1.73(1)	C3–C4	1.38(2)
S2–C2	1.72(1)	S8–C4	1.69(1)	C7–C8	1.48(4)
S3–C3	1.71(1)	S8–C6	1.72(1)		
S4–C4	1.71(1)	S9–C5	1.62(1)		
S5–C1	1.74(1)	S10–C6	1.63(1)		

S1–Ni1–S2	93.2(2)°	S1–Ni1–S3	88.1(2)°
S1–Ni1–S4	178.9(2)	S2–Ni1–S3	177.7(2)
S2–Ni1–S4	86.4(2)	S3–Ni1–S4	92.4(2)
Ni1–S1–C1	102.4(5)	Ni1–S2–C2	101.8(5)
Ni1–S3–C3	102.5(5)	Ni1–S4–C4	104.4(5)
C1–S5–C5	97.3(7)	C2–S6–C5	97.4(7)
C3–S7–C6	96.7(7)	C4–S8–C6	97.6(7)
C7–N1–C9	87(2)	C7–N1–C10	95(1)
C7–N1–C10	95(1)	C9–N1–C10	93(1)
C9–N1–C10	93(1)	C10–N1–C10	166(2)
S1–C1–S5	123.2(8)	S1–C1–C2	120(1)
S5–C1–C2	115(1)	S2–C2–S6	121.7(9)
S2–C2–C1	121(1)	S6–C2–C1	116(1)
S3–C3–S7	122.9(9)	S3–C3–C4	121(1)
S7–C3–C4	115(1)	S4–C4–S8	124.1(9)
S4–C4–C3	118(1)	S8–C4–C3	116(1)
S5–C5–S6	112.8(8)	S5–C5–S9	123.4(9)
S6–C5–S9	123.8(9)	S7–C6–S8	113.4(8)
S7–C6–S10	124.2(9)	S8–C6–S10	122.3(9)
N1–C7–C8	106(2)		

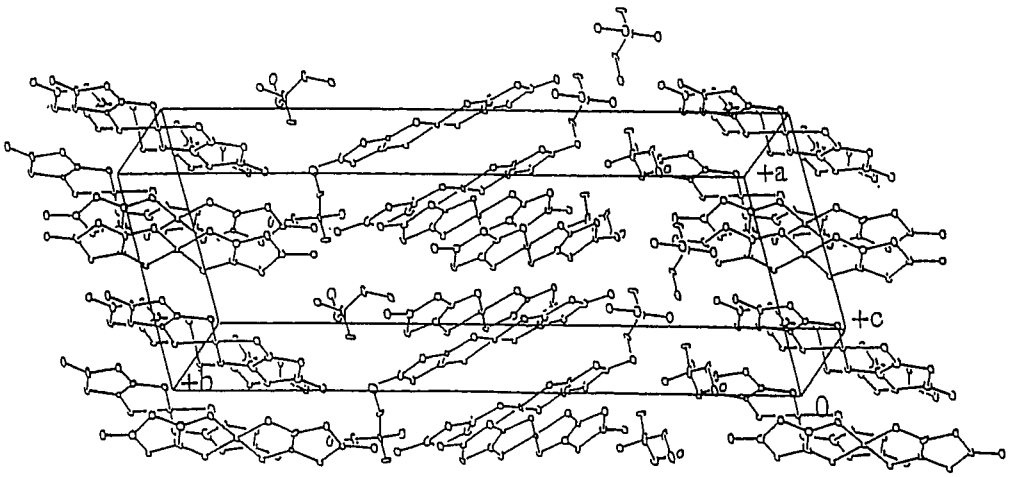

FIG. 4. The crystal structure of γ-$[(CH_3)_2(C_2H_5)_2N][Ni(dmit)_2]_2$ at 7 K. The thermal ellipsoids of ORTEP are drawn at the 50% probability level.

$[Ni(dmit)_2]_2$ was estimated as $\chi_{dia} = -4.6 \times 10^{-4}$ emu/mol. As mentioned above, the crystal structure analyses at 294 and 7 K show that there is a structural phase transition in the γ-salt. The small susceptibility decrease around 120 K indicates that the structure change takes place around 120 K. The temperature dependence of the lattice constants shown in Fig. 5 also suggests the structure change around this temperature range. The paramagnetic susceptibilities were 8.1×10^{-4} emu/mol above 120 K and 7.7×10^{-4} emu/mol below 120 K, which are comparable to those of α-BEDT-TTF_2I_3 (6.8×10^{-4} emu/mol) and β-(BEDT-$TTF)_2IBr_2$ (8×10^{-4} emu/mol) (16). As seen from Table 10, the main intermolecular overlap integrals were enhanced at low temperature, which means an increase of the band width and therefore a decrease of the Pauli paramagnetism. This may be the main origin of the decrease of the susceptibility around 120 K. Thus, the susceptibility behavior of γ-$[(CH_3)_2(C_2H_5)_2N][Ni(dmit)_2]_2$ seems to be consistent with the normal metallic properties of the system. However,

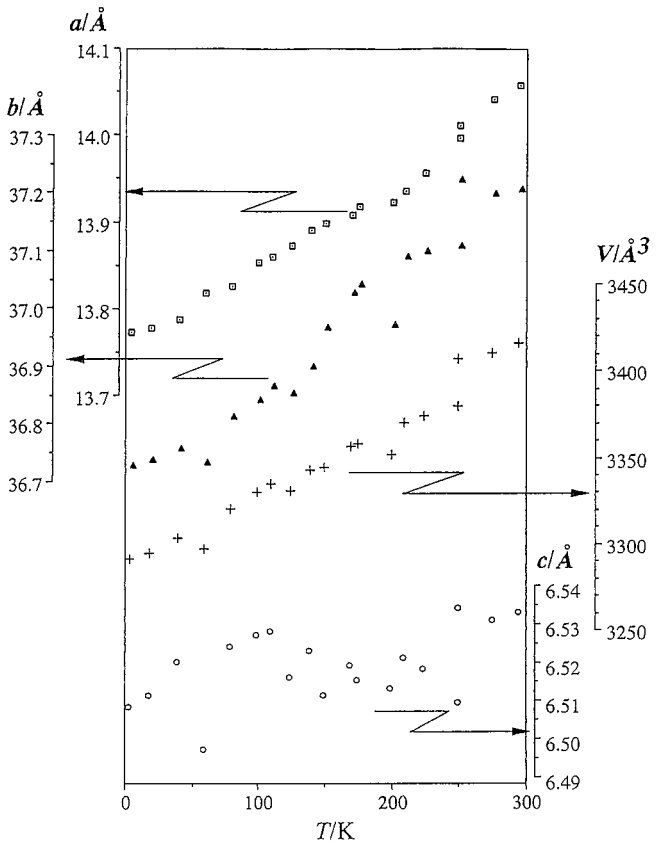

FIG. 5. The temperature dependences of the lattice constants of γ-$[(CH_3)_2(C_2H_5)_2N][Ni(dmit)_2]_2$.

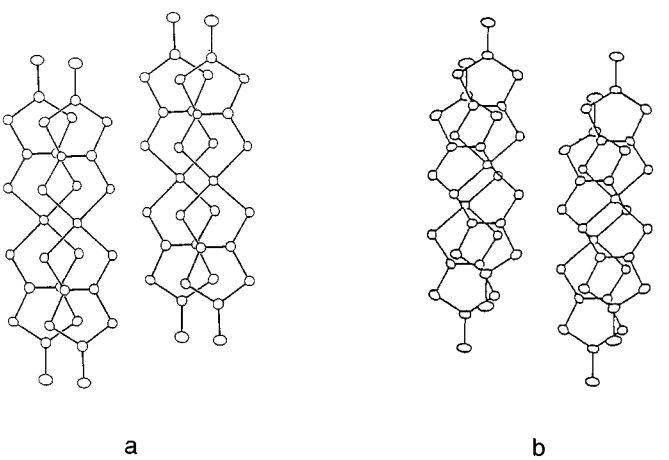

FIG. 6. The overlaps of dimers of $Ni(dmit)_2$ at 294 K in γ-$[(CH_3)_2(C_2H_5)_2N][Ni(dmit)_2]_2$ (a) and in α-$[(CH_3)_2(C_2H_5)_2N][Ni(dmit)_2]_2$ (b).

TABLE 7
Selected Bond Lengths (Å) and Angles (°) of γ-$[(CH_3)_2(C_2H_5)_2N][Ni(dmit)_2]_2$ at 7 K

Ni1–S1	2.153(12) Å	S7–C6	1.75(5) Å	S17–C9	1.74(5) Å
Ni1–S2	2.163(12)	S8–C6	1.74(5)	S18–C10	1.73(5)
Ni1–S3	2.158(13)	S9–C5	1.66(5)	S15–C11	1.75(4)
Ni1–S4	2.172(12)	S10–C6	1.63(5)	S16–C11	1.72(4)
S1–C1	1.69(5)	Ni2–S11	2.154(12)	S17–C12	1.79(5)
S2–C2	1.71(5)	Ni2–S12	2.165(13)	S18–C12	1.71(5)
S3–C3	1.73(5)	Ni2–S13	2.166(12)	S19–C11	1.65(4)
S4–C4	1.72(5)	Ni2–S14	2.154(12)	S20–C12	1.61(5)
C1–C2	1.40(5)	S11–C7	1.72(5)	N1–C13	1.51(6)
C3–C4	1.33(5)	S12–C8	1.71(4)	N1–C14	1.53(6)
S5–C1	1.72(5)	S13–C9	1.70(5)	N1–C15	1.57(5)
S6–C2	1.74(5)	S14–C10	1.66(5)	N1–C17	1.52(6)
S7–C3	1.75(5)	C7–C8	1.37(5)	C15–C16	1.49(6)
S8–C4	1.76(5)	C9–C10	1.40(5)	C17–C18	1.55(6)
S5–C5	1.74(5)	S15–C7	1.71(5)		
S6–C5	1.71(5)	S16–C8	1.75(4)		
S1–Ni1–S2	92.6(5)°	S4–C4–C3	122(4)°		
Ni1–S1–C1	104(2)	S7–C3–C4	117(4)		
Ni1–S2–C2	102(2)	S8–C4–C3	116(4)		
S1–C1–C2	120(4)	S7–C6–S8	112(3)		
S2–C2–C1	121(4)	S7–C6–S10	122(3)		
S5–C1–C2	116(4)	S8–C6–S10	125(3)		
S6–C2–C1	115(4)	C3–S7–C6	97(2)		
C1–S5–C5	96(2)	C4–S8–C6	97(2)		
C2–S6–C5	97(2)	S11–Ni2–S12	93.0(5)		
S5–C5–S6	115(3)	Ni2–S11–C7	104(2)		
S5–C5–S9	120(3)	Ni2–S12–C8	102(2)		
S6–C5–S9	125(3)	S11–C7–C8	118(4)		
S3–Ni1–S4	93.3(5)	S12–C8–C7	123(3)		
Ni1–S3–C3	101(2)	C8–C7–S15	117(4)		
Ni1–S4–C4	101(2)	C7–C8–S16	115(3)		
S3–C3–C4	122(4)	S15–C11–S16	113(2)		
S4–C4–C3	122(4)	S15–C11–S19	123(3)		
S16–C11–S19	124(3)	C10–S18–C12	100(2)		
C11–S15–C7	97(2)	S17–C12–S20	123(3)		
C11–S16–C8	97(2)	S18–C12–S20	125(3)		
S13–Ni2–S14	92.2(5)	S17–C12–S18	112(3)		
S13–C9–C10	120(4)	C13–N1–C14	110(3)		
S14–C10–C9	121(4)	C13–N1–C15	107(3)		
Ni2–S13–C9	103(2)	C13–N1–C17	115(3)		
Ni2–S14–C10	104(2)	C14–N1–C15	109(3)		
S17–C9–C10	116(4)	C14–N1–C17	106(3)		
S18–C10–C9	115(4)	C15–N1–C17	111(3)		
C9–S17–C12	97(2)				

TABLE 8
Nonbonded Contacts Less than 3.70 Å in γ-$[(CH_3)_2(C_2H_5)_2N][Ni(dmit)_2]_2$ at 294 K

S1 ⋯ S4	3.458(5) Å	S1 ⋯ S2	3.599(5) Å
S1 ⋯ S8 # 2	3.702(6)	S2 ⋯ S5	3.603(6)
S2 ⋯ S8 # 3	3.571(6)	S3 ⋯ S8	3.536(5)
S3 ⋯ S4 # 2	3.414(6)	S4 ⋯ S4 # 3	3.521(8)
S3 ⋯ S4	3.651(5)	S5 ⋯ S7 # 2	3.698(6)
S5 ⋯ S10 # 2	3.684(7)	S5 ⋯ S7 # 3	3.776(6)
S9 ⋯ S9 # 4	3.665(8)		

Symmetry operators
#2 $1/2 - x, -y, 1/2 + z$
#3 $-x, -y, -z$
#4 $x, 1/2 - y, z$

contrary to the γ-salt, the magnetic susceptibility of the α-salt showed a broad maximum around 240 K (see the inset of Fig. 7). A large susceptibility drop, related to the order–disorder phase transition, was observed around 240 K. The magnitude of the maximum magnetic susceptibilities is about 9×10^{-4} emu/mol. The round susceptibility maximum around 250 K and the gradual decrease of the susceptibility at 50–200 K suggest the existence of antiferromagnetically interacting localized magnetic moments on $Ni(dmit)_2$ molecules. Since α-$[(CH_3)_2(C_2H_5)_2N][Ni(dmit)_2]_2$ retains the metallic state, the paramagnetic susceptibility of metal electrons will remain even at low temperatures. But the paramagnetic susceptibility of α-salt becomes smaller than that of γ-salt at low temperature. Thus the strong decrease of the susceptibility of the α-salt at low temperature indicates not only diminishing of the paramagnetism due to localized magnetic moments but also the decrease of the Pauli susceptibility. The structural phase transitions accompanied with the changes of the lattice perioicities will be responsible for the decrease of Pauli susceptibility. On the contrary, the constant susceptibility of γ-phase suggests the absence of the localized magnetic moments on $Ni(dmit)_2$. The existence or absence of the localized magnetic moments on $Ni(dmit)_2$ molecules will be related to the difference of the intermolecular overlapping modes. The mode of molecular arrangements in α-salt is different from that of γ-salt at room temperature, but it becomes more similar to that of γ-phase at low temperature (17), which will give a clue to explain the puzzling con-

TABLE 9
Nonbonded Contacts Less than 3.70 Å in γ-$[(CH_3)_2(C_2H_5)_2N][Ni(dmit)_2]_2$ at 7 K

S1 ⋯ S2	3.625(15) Å	S2 ⋯ S1 # 2	3.381(15) Å
S1 ⋯ S14	3.444(15)	S3 ⋯ S18	3.48(2)
S4 ⋯ S5 # 2	3.678(15)	S5 ⋯ S12	3.52(2)
S6 ⋯ S8 # 2	3.63(2)	S7 ⋯ S17	3.78(2)
S7 ⋯ S18	3.67(2)	S8 ⋯ S9 # 2	3.67(2)
S8 ⋯ S17	3.61(2)	S10 ⋯ S19 # 4	3.576(15)
S13 ⋯ S14 # 2	3.35(2)	S15 ⋯ S17 #2	3.63(2)
S15 ⋯ S20 # 2	3.70(2)	S17 ⋯ S11 #2	3.63(2)
S18 ⋯ S11 # 2	3.67(2)		

Symmetry operators
#2 $1/2 - x, -y, 1/2 + z$
#3 $1/2 + x, 1/2 - y, -z$
#4 $-x, 1/2 + y, 1/2 - z$

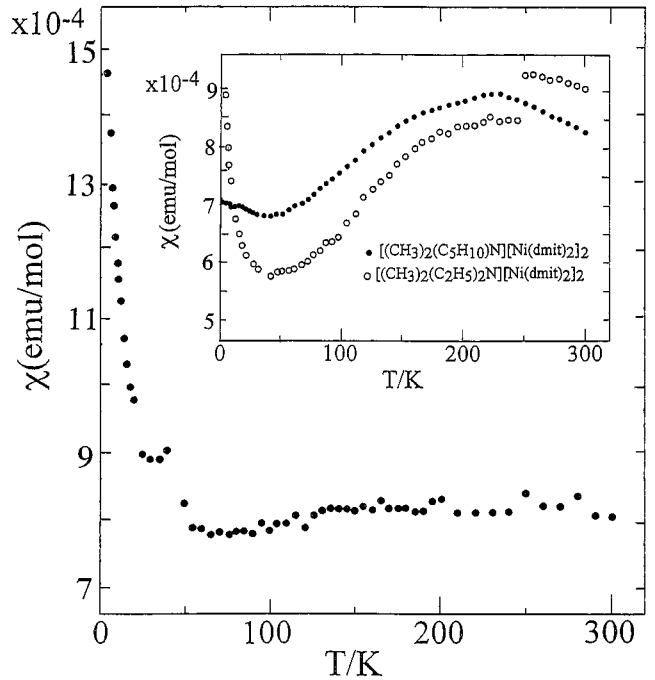

FIG. 7. Temperature dependence of magnetic susceptibility of γ-$[(CH_3)_2(C_2H_5)_2N][Ni(dmit)_2]_2$ and the inset shows those of α-$[(CH_3)_2(C_2H_5)_2N][Ni(dmit)_2]_2$ and $[(CH_3)_2(C_5H_{10})N][Ni(dmit)_2]_2$.

trastive magnetic behaviors of α-$[(CH_3)_2(C_2H_5)_2N][Ni(dmit)_2]_2$ and γ-$[(CH_3)_2(C_2H_5)_2N][Ni(dmit)_2]_2$.

Band Structure Calculation

The tight-binding band structure calculation of γ-salt at 7 K gave two-dimensional Fermi surfaces closed on the XV line due to the degeneracy of the band energies, which is almost the same as that based on the room-temperature structure (Fig. 8). Although the molecular arrangement of α-salt resembles that of γ-salt, the Fermi surface of α-salt is different from that of γ-salt. The Fermi surface of α-salt at room temperature is similar to those of κ-type organic superconductors with a two-dimensional cylindrical Fermi surface, whose close cross-sectional area is 100% of BZ (Fig. 9). As reported before (10), the tight-binding band calculation of α-salt based on the structure studies at 12 K gave complex two-dimensional Fermi surfaces which agree well with those expected from magnetoresistance experiments. This result showed for the first time that the simple extended Hückel band calculation, which had been successfully applied to organic metals, is also valid for the evaluation of the Fermi surfaces of the molecular metals based on transition-metal-complex molecules. Since γ-$[(CH_3)_2(C_2H_5)_2N][Ni(dmit)_2]_2$ retains a simple two-dimensional Fermi surface at low temperature, it might be thought to be a possible candidate of an ambient pressure π-acceptor superconductor with a closed-shell cation. However, as already mentioned, the superconductivity was not observed down to 0.1 K. Although a small Pauli susceptibility (or state density) decrease around 120 K will be unfavourable for the realization of the superconductivity, it will not be so serious. In many molecular conductors, superconducting phases seem to neighbor on the insulating phases (especially

TABLE 10
The Overlap Integrals($\times 10^3$) of γ-$[(CH_3)_2(C_2H_5)_2N][Ni(dmit)_2]_2$

(1) at 294 K
$p = 9.07$ $q = 3.50$
$A = -5.98$ $s = 0.58$
$t = 0.69$.

(2) at 7 K
$p = 10.69$ $q = 5.13$
$A = -7.16$ $s = -0.27$
$t = 0.73$

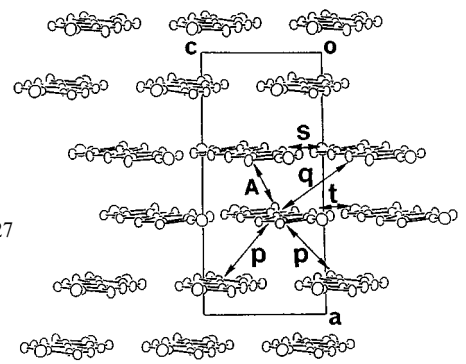

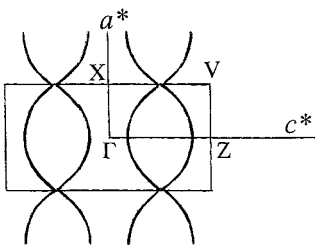

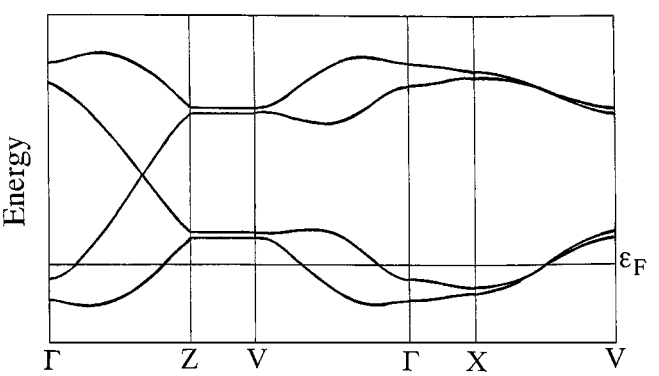

FIG. 8. The tight-binding band structure and Fermi surface of γ-$[(CH_3)_2(C_2H_5)_2N][Ni(dmit)_2]_2$.

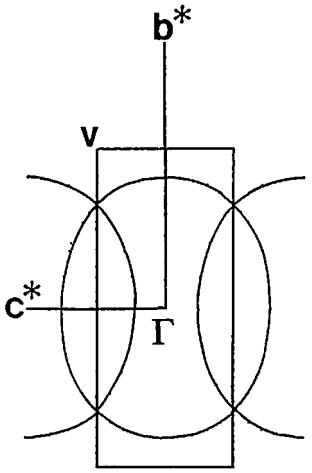

FIG. 9. The Fermi surface of α-$[(CH_3)_2(C_2H_5)_2N][Ni(dmit)_2]_2$ at 294 K.

antiferromagnetic insulating phases). This suggests that the molecular conductors with the simple stable metallic states are not good candidates of the superconductors.

In the course of trying to remove the disorderness of $(CH_3)_2(C_2H_5)_2N$ cations, we obtained $(C_7H_{16}N)[Ni(dmit)_2]_2$ ($C_7H_{16}N$ = dimethylpiperidinium) (18) having isomorphous structure to that of α-$[(CH_3)_2(C_2H_5)_2N][Ni(dmit)_2]_2$. The dimethylpiperidinium cation has a size similar to $(CH_3)_2(C_2H_5)_2N^+$ and has a more rigid conformation. Although the crystal of $(C_7H_{16}N)[Ni(dmit)_2]_2$ was metallic down to 0.5 K, no sign of superconductivity was observed also in this system. It should be also noted that the susceptibility behavior closely resembles that of α-$[(CH_3)_2(C_2H_5)_2N][Ni(dmit)_2]_2$ (see inset of Fig. 7). We should conclude that the possibility of finding the ambient-pressure pure π-acceptor superconductor with characteristic spanning overlapping molecular arrangements seems to be small.

ACKNOWLEDGMENTS

The authors thank Drs. Y. Nakazawa (IMS) and K. Kato (IMS) for the measurements of electrical conductivity of γ-$[(CH_3)_2(C_2H_5)_2N][Ni(dmit)_2]_2$ down to 0.1 K. This work was supported by a Grant-in Aid for Scientific Research on Priority Areas (No. 10149101 "Metal-assembled Complexes") from the Ministry of Education, Science, Sports, and Culture, Japan.

REFERENCES

1. P. Cassoux, L. Valade, H. Kobayashi, A. Kobayashi, R. A. Clark, and A. E. Underhill, *Coord. Chem. Rev.* **110,** 115 (1991); L. Brossard, M. Ribault, L. Valade, and P. Cassoux, *Physica B & C* (*Amsterdam*) **143,** 378 (1986); L. Brossard, M. Ribault, L. Valade and P. Cassoux, *Phys. Rev. B* **42,** 3935 (1990).
2. M. Bousseau, L. Valade, J.-P. Legros, P. Cassoux, M. Garbauskas, and L. V. Interrante, *J. Am. Chem. Soc.* **108,** 1908 (1986).
3. L. Brossard, H. Hurdequint, M. Ribault, L. Valade, J.-P. Legros, and P. Cassoux, *Synth. Metals* **27,** B157 (1988).
4. A. Kobayashi, H. Kim, Y. Sasaki, R. Kato, H. Kobayashi, S. Moriyama, Y. Nishio, K. Kajita, and W. Sasaki, *Chem. Lett.* 1819 (1987); H. Kim, A. Kobayashi, Y. Sasaki, R. Kato, and H. Kobayashi, *Chem. Lett.* 1799 (1987).
5. A. Kobayashi, H. Kobayashi, A. Miyamoto, R. Kato, R. A. Clark, and A. E. Underhill, *Chem. Lett.* 2163 (1991); A. Kobayashi, A. Miyamoto, R. Kato, A. Sato, and H. Kobayashi, *Bull. Chem. Soc. Jpn.* **71,** 997 (1998).
6. H. Kobayashi, K. Bun, T. Naito, R. Kato, and A. Kobayashi, *Chem. Lett.* 1909 (1992).
7. H. Tajima, M. Inokuchi, A. Kobayashi, T. Ohta, R. Kato, H. Kobayashi, and H. Kuroda, *Chem. Lett.* 1235 (1993); A. Kobayashi, A. Sato, K. Kawano, T. Naito, H. Kobayashi, and T. Watanabe, *J. Mater. Chem.* **5,** 1671 (1995).
8. R. Kato, Y. Kashimura, S. Aonuma, N. Hanasaki, and H. Tajima, *Solid State Commun.* **105,** 561 (1998).
9. R. Kato, H. Kobayashi, H. Kim, A. Kobayashi, Y. Sasaki, T. Mori, and H. Inokuchi, *Chem. Lett.* 865 (1988).
10. A. Kobayashi, T. Naito, and H. Kobayashi, *Phys. Rev. B. Condens. Matter* **51,** 3198 (1995).
11. A. Kobayashi, T. Naito, A. Sato, and H. Kobayashi, *Synth. Metals* **86,** 1841 (1997).
12. Crystal Structure Analysis Package, Molecular Sructure Corporation, 1985 & 1992.
13. The lowest temperature of this X-ray imaging plate system was previously reported to be 4.3 K but we have recently found the real temperature at the top of the copper needle, on which the crystals (or crystal on the gold wire) were attached by gold paint, was fairly higher than the indicated temperature. The lowest temperature in this study was about 7 K.
14. The refinement program ANYBLK was written by H. Imoto of the University of Tokyo.
15. At first, the room temperature band structure was calculated on the basis of LUMO and HOMO; however, there was no contribution from HOMO. So the band structure at 7 K was calculated withoiut HOMO.
16. J. M. Williams, J. R. Ferraro, R. J. Thorn, K. D. Carlson, U. Geiser, H. H. Wang, A. M. Kini, and M.-H. Whangbo, "Organic Superconductors (Including Fullerenes), Synthesis, Styructure, Properties and Theory." Prentice Hall, Englewood Cliffs, NJ, 1992.
17. As mentioned before, the mode of $Ni(dmit)_2$ arrangement in α-salt is different from that of γ-salt at room temperature. However, below 240 K, where a very large structural phase transition occurs, the mode of molecular arrangement of a half of $Ni(dmit)_2$ layers changes from an α-type arrangement to a γ-type one.
18. A. Kobayashi, A. Sato, T. Naito, and H. Kobayashi, *Mol. Cryst. Liq. Cryst.* **284,** 85 (1996).